

Title	COLLAPSE OF TWO-AND THREE- TORI AND APPEARANCE OF CHAOS IN DISSIPATIVE SYSTEMS(Theory of Dynamical Systems and Its Application to Nonlinear Problems)
Author(s)	Kaneko, Kunihiro
Citation	数理解析研究所講究録 (1984), 536: 160-179
Issue Date	1984-09
URL	<a href="http://hdl.handle.net/2433/98676">http://hdl.handle.net/2433/98676</a>
Right	
Type	Departmental Bulletin Paper
Textversion	publisher

# COLLAPSE OF TWO- AND THREE- TORI AND APPEARANCE OF CHAOS IN DISSIPATIVE SYSTEMS

Kunihiko Kaneko (金子 邦彦)

Department of Physics, Faculty of Science,  
University of Tokyo  
Hongo, Bunkyo-ku, Tokyo 113

## ABSTRACT

Collapse of tori in dissipative systems are investigated with the use of mappings. First, phase instability of a two-torus is studied by the circle map. Similarity and scaling properties of lockings are summarized. Supercritical behavior on the disordering property of chaos and on the speed of the collapse of a torus is characterized by the crossover exponent. Secondly, amplitude instabilities of tori, such as fractalization and torus doubling are briefly shown. Lastly, stability of a three-torus is shown by the numerical study on the coupled circle map. Chaos appears even for a weak-coupling. The mechanism of its onset is discussed.

## 1. Introduction

Appearance of chaos through quasiperiodic motion has been observed in a variety of dissipative nonlinear systems, such as Rayleigh-Bénard convection, Taylor instability, and Josephson junction. Though the studies in Hamiltonian systems have made clear the various aspects on the collapse of a KAM torus, the collapse of a torus in dissipative systems has not yet been well understood and the mechanism of the onset of chaos has remained to be an important problem in nonlinear science. We can classify the mechanism which has been known so far, as follows:

### A) From $T^2$

- 1) Phase instability  $\implies$  " chaos through locking (circle map)"
- 2) Amplitude Instability
  - a) Fractalization  $\implies$  " onset of chaos through fractal torus"
  - b) Doubling of Torus  $\implies$  " a finite number of times of doubling"
  - c) Torus Intermittency

### B) From $T^3 \implies$ " Stability of $T^3$ and double devil's staircase"

In the present paper we study the various instabilities of two- or three-tori and study the mechanism of the appearance of chaos. The construction of the paper is as follows:

In §2, the phase instability of  $T^2$  is studied by the circle map. After summing up the previous result for the circle map, we investigate the supercritical behavior after the collapse of tori. We characterize the chaotic motion by introducing the notion of "disordering". Speed of the collapse of a torus is also studied.

In §3, the amplitude instabilities of  $T^2$  are briefly summarized. Especially the fractalization and doubling of a torus is explained.

In §4, stability of  $T^3$  is studied with the use of the coupled circle map. The large difference between  $T^3$  and  $T^2$  is its stability. Though,  $T^3$  stably exists for a finite coupling, chaos appears in the neighborhood of  $T^3$  even for a weak-coupling system. The measure of various attractors in the parameter space and the onset of chaos are investigated.

Since the pages are limited, details are omitted, which are seen in the references and in the PhD thesis by the author (1983, Univ. of Tokyo).

## 2. Phase Instability

### a) Circle Map

If the instability in the phase motion of a torus is a relevant mechanism of the collapse of tori, a one-dimensional map for the phase motion is a useful tool. The typical model is the circle map<sup>2)-12)</sup>

$$x_{n+1} = x_n + A \sin(2\pi x_n) + D. \quad (2.1)$$

For  $A < A_c = 1/(2\pi)$ , the map is invertible and the attractor is a torus or a cycle, while the attractor is chaos or a cycle (window) for  $A > A_c$ . The rotation number of the map is defined by  $\lim_{n \rightarrow \infty} (x_n - x_0)/n$ , which is rational for a cycle (locking) and irrational for a torus. The rotation number as a function of  $D$  forms an incomplete devil's staircase for  $A < A_c$ . Following aspects have been elucidated by recent studies<sup>2)-12)</sup>.

1) Critical phenomena at  $A \rightarrow A_c = 0$ : A torus is approximated by a sequence of lockings with the rotation number which is obtained by the continued fraction expansion for an irrational rotation number<sup>19)</sup>. The convergence of the approximation in the parameter space  $D$  and in the phase space  $x$  shows a remarkable change at  $A = A_c$ . The scalings for the convergence rate are characterized by two exponents, which take nontrivial values at  $A = A_c$ <sup>2)</sup>. The values are consistent with the RG theory<sup>3)4)</sup> and Feigenbaum's theory for the period-doubling<sup>13)</sup>.

2) A "period-adding" sequence of cycles (lockings or windows) is easily observed in numerical and real experiments, since it has a large stability. Let us take a sequence of lockings with a period  $(pn+r)$  with the rotation number  $(qn+s)/(pn+r)$ . If we define  $A_n$  ( $A_n^f$ ) by the parameter value at which the  $(pn+r)$ -cycle appears (disappears), scaling relations  $A_n - A \propto n^{-2}$  and  $A_n^f - A_n \propto n^{-3}$  hold. Furthermore, the sequence has a similarity, which is expressed by the existence of a fixed point function for the scaled Lyapunov exponent. The scalings are explained by the tangent bifurcation theory<sup>14)</sup>, while the form of the scaled Lyapunov exponent is derived by a phenomenological theory based on the fixed-point function ansatz. The similarity of the period-adding sequence is seen both for  $A > A_c$  and  $A < A_c$ . The difference between the two regions are expressed by the form of the scaled Lyapunov exponent<sup>5)</sup>. (The period-adding sequence appears not only in frequency lockings but also in a variety of systems, for example, in connection with the intermittent transition<sup>5)</sup>, homoclinic orbits<sup>15)</sup> and crisis<sup>12)</sup>. The framework of the similarity theory in Ref.5) can easily be extended to these cases.)

3) The measure of the lockings in the parameter space  $D$  becomes unity at  $A = A_c$ . They form a complete devil's staircase<sup>9)</sup>.

4) The windows for  $A > A_c$  show a similarity structure, which is analyzed by the locus of superstable orbits<sup>7)</sup> and the above period-adding study.

5) The number of the attractors is unity for  $A < A_c$ , while it increases up to two for  $A > A_c$  and bistability can appear<sup>5)8)12)</sup>.

In the subsections b) and c) we study the property of chaotic orbits for  $A > A_c$ .

### b) Disorderings

The remarkable difference between chaotic and torus orbits is whether the orbit is ordered or not. For a torus orbit, two nearby orbits do not change their order, i.e.,  $x_n > x'_n$  if  $x_0 > x'_0$ . On the other hand, two nearby orbits change their order for a chaotic orbit, if the orbits fall on the interval  $I = \{x | f'(x) < 0\}$ . We define the disordering ratio by  $d = \int_I \rho(x) dx$  where  $\rho(x)$  is the invariant measure. Since the disordering property is brought about by the interval  $I$ , it is useful to introduce the following induced map  $F(x)$ <sup>17)</sup> in the region  $I$ ;

$$F(x) = f^k(x); \quad k = \text{minimum integer such that } f^k(x) \in I \quad (2.2)$$

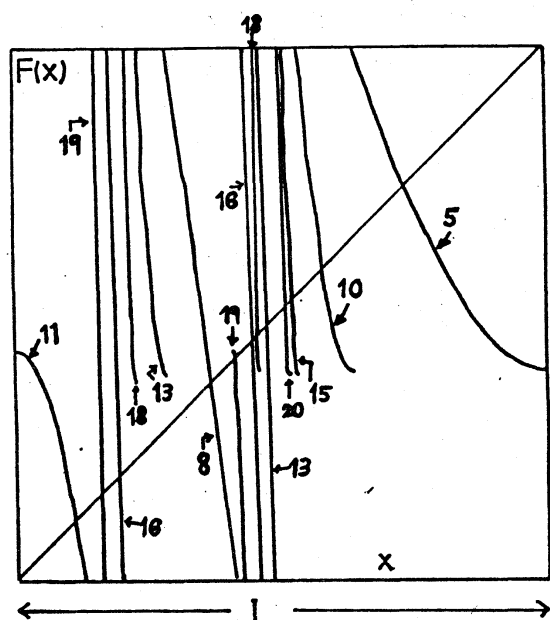


Fig.1 Induced map  $F(x)$  (see Eq. (2.2)) with the disordering time  $k$ , where the time  $k$  is shown up to 20.  $A=0.2058$  and  $D=0.6$ .

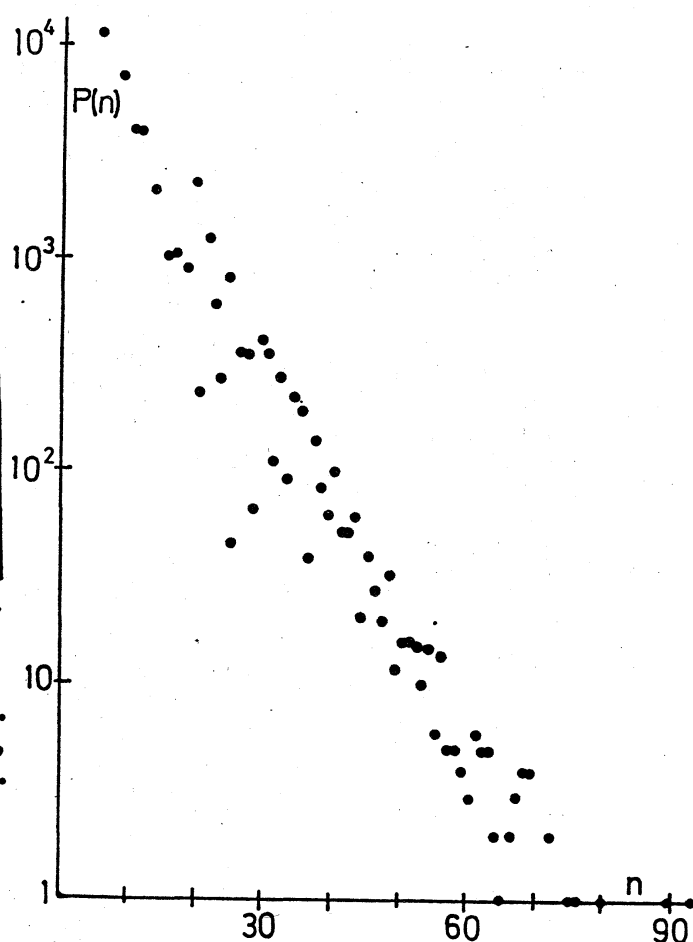


Fig.2

Distribution of disordering times  $P(n)$ , which is obtained from 50000 iterations of the circle map with the same parameter as the ones in Fig.1. (Initial 10000 iterations are dropped.)

It is also useful to introduce the disordering time distribution  $P(k)$  for one orbit with a long time average, i.e.,

$$P(k) = \frac{\int_{x \in I_k} \rho(x) dx}{\int_{x \in I} \rho(x) dx}, \quad (2.3)$$

where  $I_k \subset I$  is the region such that  $f^k(x) \in I$  and  $f^m(x) \notin I$  for  $m < k$ .

An example of an induced map and a disordering time distribution is given in Fig.1 and Fig.2. We have obtained the induced map and the distribution at various parameter values  $A$  and  $D$ . The following points should be noted.

1) Chaos with the disordering ratio  $2/(3p)$  appears through a period-doubling cascade from a  $p$ -cycle (see for the phase diagram Fig.3). As  $A$  is increased further, disordering times  $p_n$  ( $n=1,2,3, \dots$ ) successively

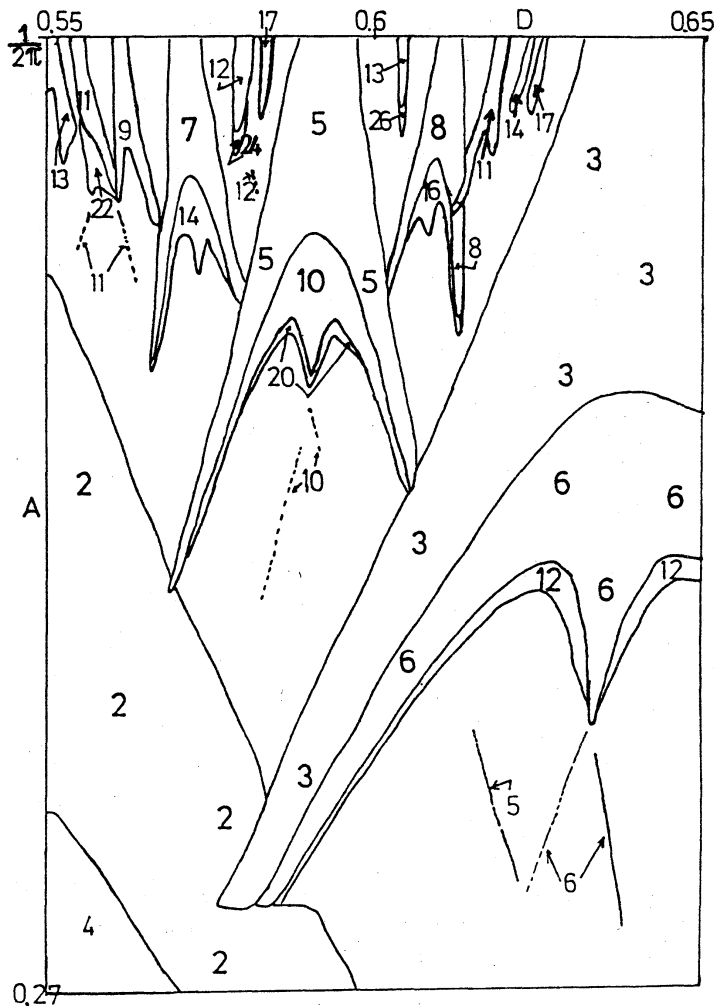


**Fig.3**  
Rough phase diagram for the circle map. Numbers in the figure denote periods, while chaos exists in the region without numbers. Small structures, such as cycles with periods larger than 26 are omitted. (Initial values of the map are  $x_0=0.5$ .)

appear till the crisis<sup>16)</sup> of a  $p$ -band chaos occurs, where  $P(pn)$  shows the behavior of  $c^{-n}$ , with  $c$  a constant.

2) As  $A$  is increased further beyond the crisis point of a  $p$ -band chaos, a new disordering time (e.g.,  $q$ ) appears. In this case, disordering times with  $pn+qm$  ( $n,m=1,2,3,\dots$ ) are apt to exist. Thus, the chaos in that region can be regarded as the mixture of  $p$ -band chaos and  $q$ -band chaos, each of which appears from a period-doubling cascade and is chaos with the type of the logistic map. As the nonlinearity  $A$  is increased, various disordering times appear and various band chaos mixes.

3) The disordering time distribution  $P(k)$  decays exponentially as a function of  $k$ , which is due to the Markov property of the map. The decay rate is related with some average of  $f'(x)$ . Thus the decay rate increases as the increase of  $A$ .

4) It is also important to construct a symbolic dynamics from the above induced map.<sup>18)</sup>

### c) Supercritical Similarity

Though the critical phenomena just below the onset of chaos from a torus motion (i.e.,  $A \rightarrow A_c - 0$ ) has been investigated extensively, the critical property just above the onset of chaos has not yet been studied. In the present subsection we consider this problem<sup>12)</sup>.

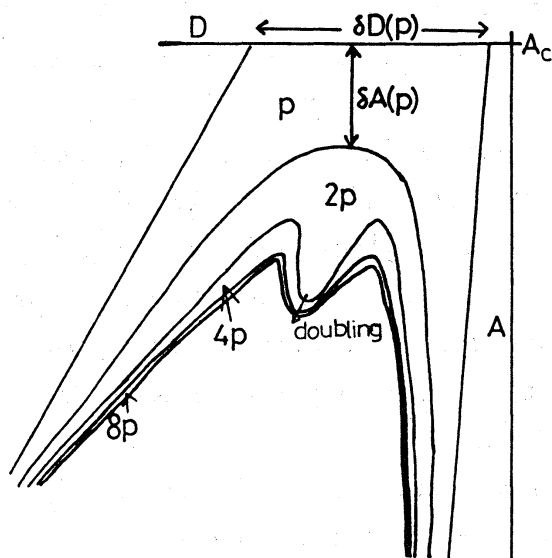


**Fig.4**

Schematic representation of the Arnold tongues for  $A > A_c$ . Each  $p$ -cycle period-doubles and chaos appears. The scales of the tongue are characterized by  $\delta A(p)$  and  $\delta D(p)$ .

Let us look at Fig.3 in more detail. Chaos appears as a period-doubling from a basic cycle  $p$ . Each of the doubling cascades in the parameter space shows a shape like Fig.4, which is similar for various basic cycles. The similarity is characterized by two scales (one for  $A-A_c$  and the other for  $D$ ) shown in the figure as  $\delta A(p)$  and  $\delta D(p)$ .

In order to consider the onset of chaos from a torus with a rotation number  $r$ , we make a rational approximation for  $r$  using the continued fraction expansion  $r_k = 1/(n_1 + 1/(n_2 + 1/\dots + 1/n_k))$  and consider the period-doubling cascade from the  $r_k$ -cycle. For a torus with the rotation number  $r$ , let us define  $\delta A_k$  and  $\delta D_k$  by  $\delta A(r_k)$  and  $\delta D(r_k)$ . The onset of chaos from the torus can be understood as the doubling of the  $r_k$ -cycle with the limit of  $k \rightarrow \infty$ . Since  $\delta A_k \rightarrow 0$  as  $k \rightarrow \infty$ , chaos appears immediately at  $A=A_c$  for the torus. The measure for a torus in the parameter space  $D$ , however, vanishes as  $A \rightarrow A_c$ . Thus, the measure of chaos in the parameter space increases rather slowly as the increase of  $A$ .

As an example we consider the torus with the rotation number  $(\sqrt{5}-1)/2$ . The rational approximation is given by  $F_k/F_{k+1}$ , where  $F_k$  is the Fibonacci sequence. Numerical calculations show that

$$\begin{aligned}\delta A_k &\propto F_k^{-\nu} \\ \delta D_k &\propto F_k^{-\gamma}\end{aligned}$$

where  $\nu$  and  $\gamma$  take the values  $1.055(\pm 0.01)$  and  $2.165(\pm 0.01)$  respectively. The value  $\gamma$  agrees with Shenker's value<sup>2)</sup>, though the definition is a little bit different. For the golden mean torus, the similarity of the "tongues" in Fig.3 and Fig.4 is characterized by the above two exponents.

The value  $\nu$  agrees with the crossover exponent found by Shenker<sup>2)</sup> for the subcritical region. If the fixed point of the RG<sup>3)4)</sup> is a saddle, it is expected that the critical indices for sub- and super-critical regions take a same value. Thus, the above agreement is rather natural. The important point is a new interpretation of the exponent  $\nu$ . It represents the **speed of the collapse of a torus**, as is seen from our definition and the arguments as follows.

Let us consider the disordering property again. When the  $F_k$ -band chaos shows a crisis, the disordering time distribution obeys



$$P(nF_k) \propto P(F_k) \times b^{-n}$$

where  $b$  is the instability exponent  $b = \prod_{i=1}^{F_k} f'(x_i)$  ( $x_i$ 's ( $i=1,2,\dots,F_k$ ) are the unstable periodic points which cause the crisis). According to the similarity in the present section,  $b$  is expected to approach a constant value as  $k \rightarrow \infty$ . Thus, the decay rate of the disordering time distribution is given by  $-(1/F_k) \log b$ . As  $A$  goes to  $A_c$ , the above study of critical phenomena shows that  $F_k$  may be replaced by  $(A-A_c)^{-\nu}$  in the parameter space. Thus the slope of the distribution goes to zero in proportion to  $(A-A_c)^{\nu}$ , as  $A$  approaches  $A_c$ . The vanish of the decay rate for the exponential damping at the critical point is universally seen in critical phenomena in general.

If the similarity argument is valid, the chaos with  $F_k$ -band is similar to the chaos with the  $F_{k+1}$ -band, and the Lyapunov exponent is proportional to  $1/F_k$ . Thus, the scaling behavior with  $(A-A_c)^{\nu}$  is again expected for the collapse of the golden mean torus.

In computer experiments (and of course in real experiments) it is rather difficult to tune the parameters  $D$  and  $A$  in the supercritical region so that the rotation number is the inverse of the golden mean. The detailed numerical check for the above critical phenomena, therefore, has not yet been carried out. In Fig. 5, the disordering time distributions are shown, where the rotation number is close to the inverse of the golden mean (though the rotation numbers in these two figures do not coincide with each other). The decrease of the slope as the decrease of  $(A-A_c)$  is clearly seen, though, of course, the distributions are not similar in the rigorous sense. The decrease of the slope is roughly proportional to  $(A-A_c)^1$  (cf.  $\nu=1.05\dots$ ). Thus, the above argument on the critical phenomena gives a rough estimate for the decrease of the slope, even if the parameters are not correctly chosen so that the similarity holds.

Figure 6 shows the increase of the Lyapunov exponent as a function of  $(A-A_c)$ . The max  $L$  in the figure represents the maximum of the Lyapunov exponent  $L(D)$  for  $0.606 < D < 0.607$ , where the rotation number of the map is close to  $(\sqrt{5}-1)/2$ . Numerically, the max  $L$  was obtained as the maximum of  $L(0.606+2i \times 10^{-5})$  with  $i=1,2,\dots,50$ . If the small dips

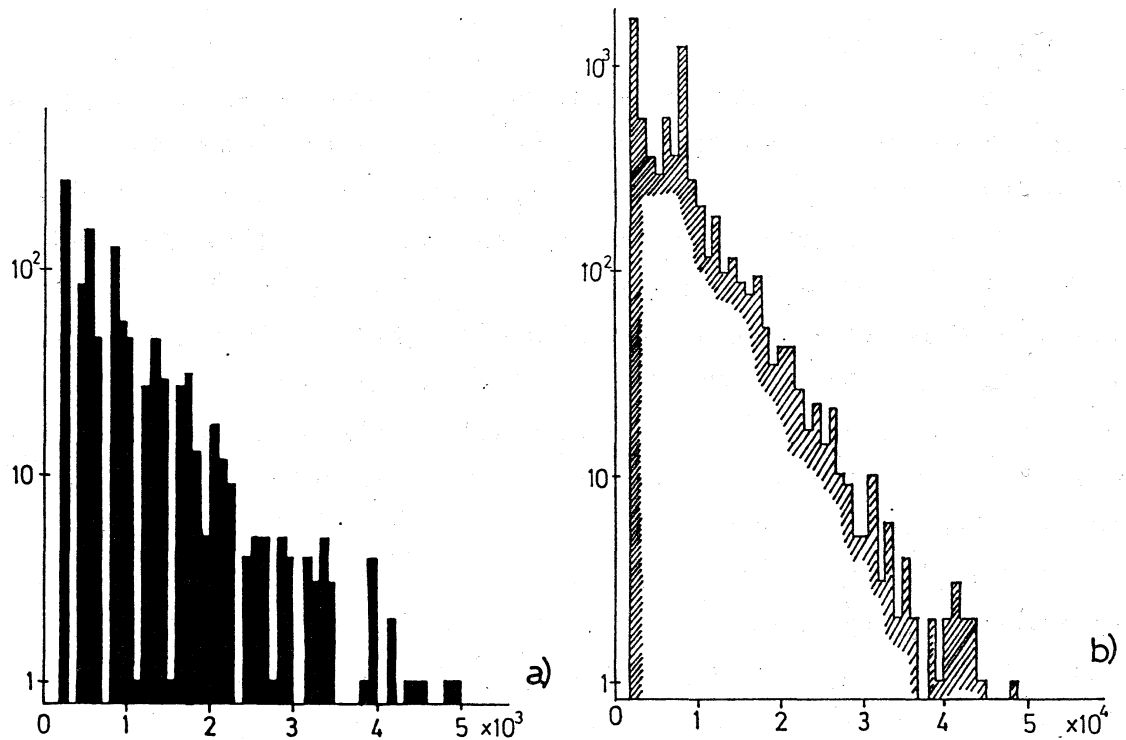


**Fig.5** Histogram of the distribution of disordering times  $P(n)$ , which is obtained from  $10^7$  iterations of the circle map. (Initial  $10^4$  iterations are dropped.)

a)  $A = A_c + 0.0008$  and  $D = 0.6065$ ; Longitudinal axis is the summation of  $P(n)$  for the interval  $(n \times 10^2, (n+1) \times 10^2)$ .

b)  $A = A_c + 0.0001$  and  $D = 0.6066$ ; Longitudinal axis is the summation of  $P(n)$  for the interval  $(n \times 10^3, (n+1) \times 10^3)$ .

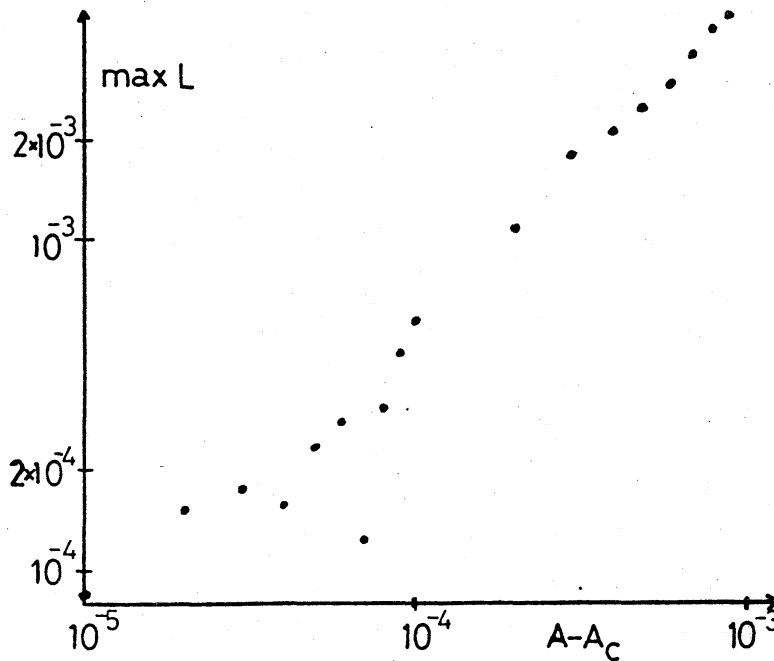


**Fig. 6**

Maximum of the Lyapunov exponent  $L(D)$  for  $0.606 < D < 0.607$  as a function of  $A$ . Lyapunov exponent was calculated from the data  $x_n$ 's of the map (2.1) for  $10^4 < n < 6 \times 10^4$ , with the initial value  $x_0 = 0.5$ .

are neglected, the increase of  $\max L$  is roughly proportional to  $(A-A_c)$ , which again justifies the above argument on the supercritical behavior.

Owing to these considerations, the exponent  $\nu$  may be regarded as the index for the speed of the collapse of a torus and the development of chaos. Shenker's numerical result for the subcritical region shows that  $\nu$  depends on the character of the tail of the continued fraction expansion of an irrational rotation number. His result shows that the exponent  $\nu$  for the rotation number with the tail  $1/(2+1/(2+1/\dots))$  is  $1.0476\dots^{2)}$ , which is smaller than the exponent for the (inverse of the) golden mean. Thus the golden mean torus collapses **faster** than the torus with the rotation number  $1/(2+1/(2+1/\dots))$ , which is contrary to the well-established result for the standard mapping where the golden mean torus is the last KAM to collapse<sup>19)</sup>. It will be of interest to check whether the conjecture is true that **the golden mean torus is the first to collapse in dissipative systems.**

### 3. Amplitude Instability

In real systems, the instabilities exist both in phase and amplitude dynamics. Phase instability induces a locking to a cycle, while the amplitude instability brings about the oscillatory behavior of a torus. The oscillation is seen in a variety of two-dimensional mappings<sup>20)21)</sup>. Since the phase instability also exists in a generic two-dimensional mapping, lockings to cycles mask the oscillation. In order to extract only the amplitude dynamics, the following (nongeneric) modulation mapping

$$\begin{aligned} x_{n+1} &= f(x_n) + K \sin(2\pi y_n) \\ y_{n+1} &= y_n + c \pmod{1} \end{aligned} \quad (3.1)$$

is useful<sup>22)23)</sup>. As  $K$  is increased, the oscillation of a torus becomes stronger till the torus is **fractal** at  $K=K_c$ <sup>22)</sup>. For  $K>K_c$ , chaos with a belt-like attractor appears. The area of the attractor increases as the increase of  $K$ . Fractalization of torus is seen in various types of  $f(x)$  (such as  $1-ax^2$ ,  $-ax+bx^2$ , and  $a\sin(2\pi x)$ ). The fractal dimension depends on the property of an irrational number  $c$  (i.e., the tail of the

continued fraction expansion of  $c$ ) but it seems to be independent of the choice of  $f(x)$ <sup>22)</sup>.

Another important instability in amplitude dynamics is torus doubling, which was discovered independently by Franceshini<sup>26)</sup>, Arneodo et al.<sup>24)</sup>, and the author<sup>21)25)</sup>. The most remarkable difference from usual period-doubling of a cycle is that the doubling of torus occurs only a finite number of times before chaos appears<sup>25)</sup>. Thus the period-doubling cascade is unstable in the torus motion. In other words, the fixed point function of the RG transformation by Feigenbaum<sup>13)</sup> is unstable against the modulation with an incommensurate period<sup>25)27)</sup>. When the doubling stops and chaos appears, the oscillatory behavior of a torus is remarkably seen. Thus, the fractalization of a torus seems to be a cause of the stop of the doubling.<sup>21)</sup>

Recently, another instability, torus intermittency has been investigated by Daido<sup>28)</sup>, where the modulation mapping of the type (3.1) is also used.

#### 4. Chaos from $T^3$

Stability of a three-torus and appearance of chaos has been an important problem since the pioneerig work by Ruelle and Takens<sup>1)</sup>. Recently the author studied some 4-dimensional mappings and showed the following aspects numerically<sup>30)</sup>

- 1) Three-torus exists for a finite coupling. As the coupling is increased, it becomes feasible to phase-lock, to produce a 2-torus.
- 2) Chaos appears through a locking to a cycle. That is, chaos appears via two steps of lockings, i.e.,  $T^3 \rightarrow T^2$  cycle  $\rightarrow$  chaos. The onset of chaos due to the Hopf-bifurcation to  $T^3$  cannot be observed.
- 3) Rotation number as a function of a bifurcation parameter forms a double-devil's staircase, which is analyzed by a coupled circle map.

Here, we consider the phase motion of a three-torus in a little more detail. A typical model is given by the coupled circle map

$$\begin{aligned} x_{n+1} &= x_n + r_x + A \sin(2\pi x_n) + B \sin(2\pi y_n) \\ y_{n+1} &= y_n + r_y + C \sin(2\pi x_n) + D \sin(2\pi y_n) \end{aligned} \quad (4.1')$$

A nongeneric case for the coupled circle map ( $C=D=0$ ) is investigated by the author<sup>30)</sup> and by Sethna and Siggia<sup>23)</sup>, while the case with higher harmonics (randomly chosen) is studied by Grebogi et al.<sup>29)</sup>. Here we reduce the number of parameters by taking  $A=D=a/2\pi(>0)$  and  $B=-C=ab/2\pi$  and  $r_x=r_y=d$ . Thus, the map (4.1') is simplified to

$$\begin{aligned} x_{n+1} &= x_n + d + a(\sin(2\pi x_n) + b\sin(2\pi y_n)) / (2\pi) \\ y_{n+1} &= y_n + d + a(\sin(2\pi y_n) - b\sin(2\pi x_n)) / (2\pi). \end{aligned} \quad (4.1)$$

The Jacobian of the map is given by

$$1 + a(\cos 2\pi x + \cos 2\pi y) + a^2(1 + b^2)\cos 2\pi x \cos 2\pi y,$$

the minimum of which is  $1 - 2a + a^2(1 + b^2)$  for  $a < 1/(1 + b^2)$  and  $1 - a^2(1 + b^2)$  for  $a > 1/(1 + b^2)$ . Thus, the map (4.1) is invertible for  $a < a_c = 1/\sqrt{1 + b^2}$ . If the coupling  $b$  vanishes, the map reduces to two independent circle maps with identical parameters. According to §1, the attractor in this case is cycle~~cycle~~ or  $T^2$  or  $T^3$  for  $a < a_c$  and cycle~~cycle~~ or chaos~~chaos~~ for  $a > a_c$ . As the coupling is increased, direct product states can become unstable.

The attractor of the map (4.1) is classified by the signs of Lyapunov exponents  $L_1$  and  $L_2 (< L_1)$ . It is  $T^3 (L_1=0, L_2=0)$ ,  $T^2(0, -)$ , cycle $(-, -)$  or chaos $(+, -$  or  $0)$  for  $a < a_c$  and  $T^2$ , cycle, chaos, or hyperchaos $(+, +)$  for  $a > a_c$ . Here we note that Ruelle and Takens' result<sup>1)</sup> does not imply the nonexistence of  $T^3$ . The numerical result for the map (4.1), on the contrary, shows that  $T^3$  has a large measure in the parameter space  $(d, b)$  for small  $a$ . The remarkable difference between  $T^3$  and  $T^2$  is that chaos exists even for  $a < a_c$  (i.e., in the invertible regime), while chaos never appears in the invertible regime for the one-dimensional circle map (2.1) for  $T^2$ .

It is a little bit difficult to distinguish  $T^3$ ,  $T^2$ , and chaos accurately by numerical methods. We calculated the two Lyapunov exponents  $L_1$  and  $L_2$  for the map with  $b=0.1$ , by iterating the map (4.1)  $3 \times 10^4$  times after dropping initial  $10^4$  times of iterations. We change the parameter  $d$  by 0.0005 for  $0 < d < 0.5$  for a given  $a$  (thus,  $10^3$  points of  $d$ 's are chosen) and counted the number of  $T^3$ ,  $T^2$ , cycle and chaos.

Here, the Lyapunov exponent is regarded as zero if its magnitude is less than  $10^{-4}$ . The ratios of the four types of attractors (i.e., the number of the parameter  $d$  at which each attractor appears, divided by  $10^3$ ) are shown in Fig. 7.

For small  $a$ , the magnitude of Lyapunov exponents is small in general, if it is regarded as to be nonzero and the distinction of attractors by the above criterion is not accurate. Especially it is difficult to distinguish  $T^3$  from  $T^2$  with small negative  $L_2$ . Thus the results for  $a \leq 0.5a_c$  cannot be taken seriously. For example, the existence of chaos at  $a \leq 0.7a_c$  cannot be confirmed from this calculation, because the magnitude of the positive Lyapunov exponent in the region

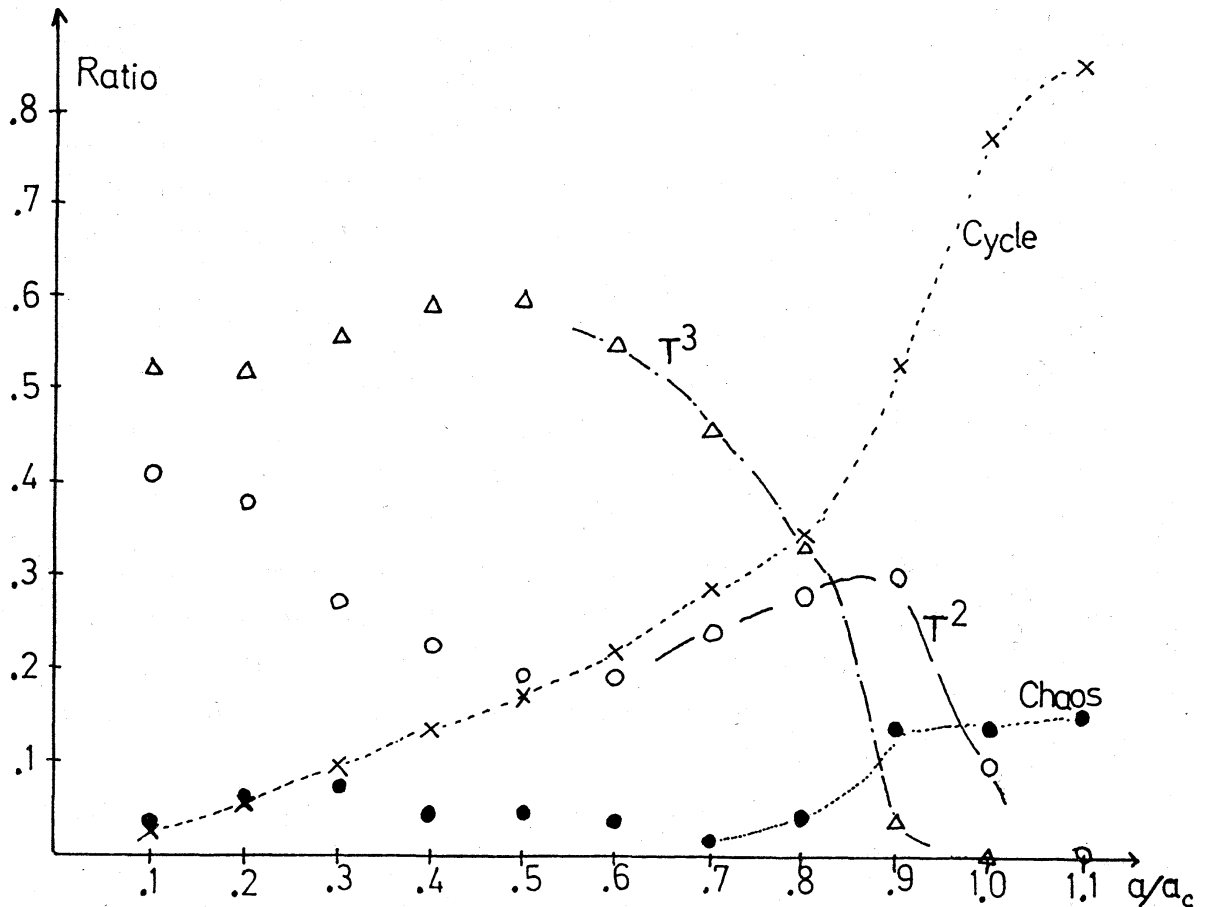
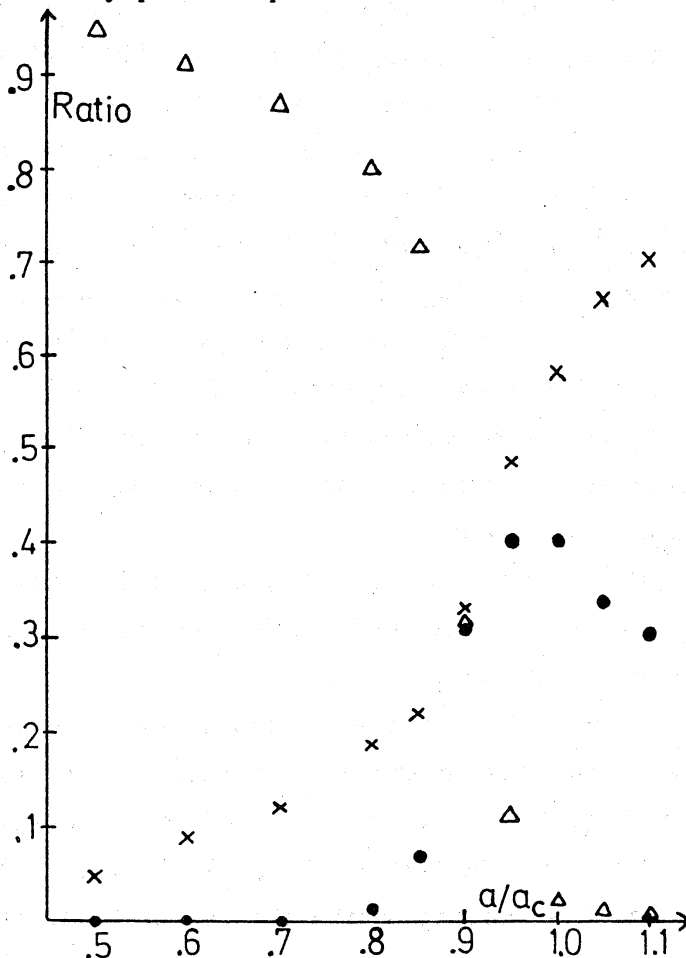


Fig. 7 The ratios of attractors  $T^3(\Delta)$ ,  $T^2(\circ)$ , cycle( $\times$ ), and chaos( $\bullet$ ), in the parameter space  $d$  as a function of  $a$ . Lines are written only for convenience. Initial values of the map (4.1) are  $(x_0, y_0) = (0, -0.02)$ .

$a \lesssim 0.7a_c$  is small ( $\sim 10^{-4}$ ) and the times of iterations may not be sufficient to make an accurate estimate of the Lyapunov exponents. Furthermore, the increase of the measure of  $T^2$  for small  $a$  might also be due to the lack of iterations.

In order to distinguish chaos from a torus more accurately, we calculated only the first Lyapunov exponent from the  $10^5$  times iterations of the map, after the initial  $10^4$  times of the transients are dropped. The parameter  $d$ 's take the values  $0.3 + 2 \times 10^{-4}i$  ( $i=1,2,3,\dots,500$ ) (i.e.,  $0.3 < d < 0.4$ ) and the ratio of each attractor is calculated as a function of  $a$  with the use of the same 'zero criterion' as for the previous figure. The ratios are shown in Fig.8, where only the ratios for a cycle, chaos, and a torus (sum of the ratios for  $T^2$  and  $T^3$ ) are shown, since it is impossible to distinguish  $T^3$  from  $T^2$  only from the first Lyapunov exponent.



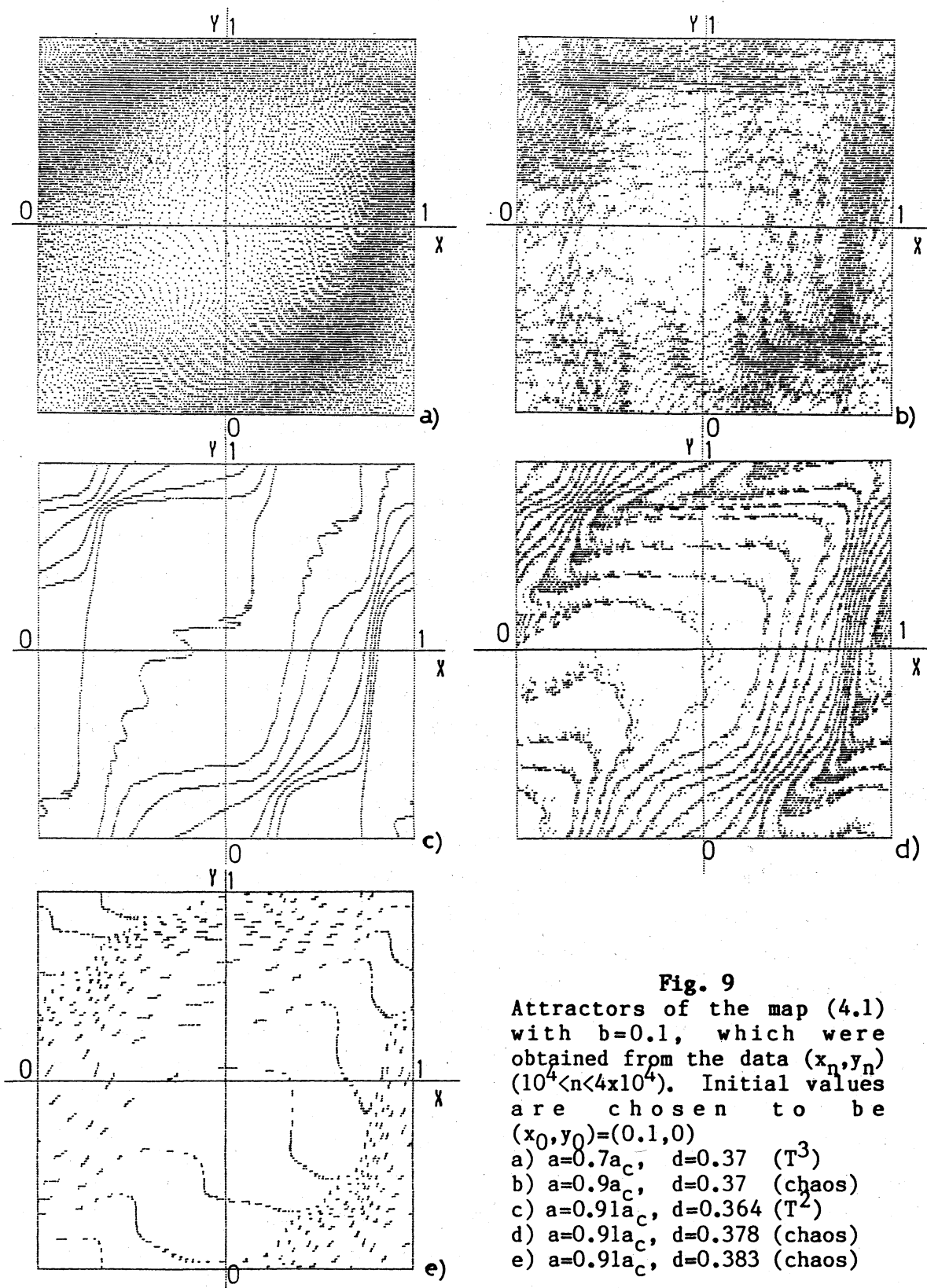
**Fig. 8**  
The ratios of attractors, tori( $T^2$  or  $T^3$ )( $\Delta$ ), cycles( $\times$ ), and chaos( $\bullet$ ), in the parameter space  $d$  as a function of  $a$ , which were obtained from the calculation of the first Lyapunov exponent for the map (4.1) with the initial values  $(x_0, y_0) = (0, -0.02)$ .

The following aspects can be seen from Figs. 7 and 8.

- 1)  $T^3$  stably exists even for a system with a finite coupling and a finite nonlinearity. The ratio is rather large for a weakly nonlinear system. It decreases as the increase of  $a$  and vanishes at  $a=a_c$ .
- 2) Lockings to cycles increase as  $a$  approaches  $a_c$ . The increase is the most remarkable change as a function of  $a$ , which can be seen from Fig. 7. Though the ratio of lockings is less than unity at  $a=a_c$  owing to the existence of chaos, it is the largest among the ratios for the four types of attractors. In this sense, lockings play a major role for the instability and disappearance of a three-torus.
- 3) Chaos appears even for  $a < a_c$ . Its measure, however, is very small for small  $a$ . According to the second calculation (for Fig. 8) chaos was not found for  $a < 0.7a_c$ . Here we note that the measure of chaos is larger in the region  $0.3 < d < 0.4$  (i.e., the region for Fig. 8) than in other regions of  $d$  according to the first calculation (for Fig. 7). Thus, it may be concluded that the measure of chaos for  $a < 0.7a_c$  is small ( $< 1/500$ ) if it exists stably in the region. In other words, chaos of Ruelle and Takens' type<sup>1)</sup> cannot be observed for  $a < 0.7a_c$ . The result agrees with the simulation of 4-dimensional mappings<sup>30)</sup>, where chaos cannot be observed in the parameter region where  $T^3$  is dominant. We cannot, of course, deny the mathematical existence of chaos for  $a < 0.7a_c$  by numerical methods. It may be concluded, however, that chaos does not exist "physically" in the weakly nonlinear (or coupled) region where  $T^3$  is dominant. We also note that the ratio of chaos shows a significant change at  $a \sim 0.85a_c$ , where lockings to cycles also increase, which seem to be essential to the appearance of chaos.
- 4) The ratio of lockings to  $T^2$  increases at  $a \sim 0.7a_c$ , but it decreases for  $a > 0.9a_c$ , where lockings to cycles increase rather rapidly. The ratio of  $T^2$ , however, does not vanish for  $a \sim 1.1a_c$ .

In Figs. 9, some examples of attractors are shown. We note the oscillatory behavior of  $T^2$  and localized attractors of chaos. Lockings exist at the parameter values close to the values for the chaos. The chaos has a large measure near the points  $(x_i, y_i)$  ( $i=1, 2, \dots, N$ ) which are the periodic points of the lockings (with the period  $N$ ) at the





nearby parameter.

It is important to note that the attractor of the map (4.1) is not always unique even for  $a < a_c$  (for the circle map (2.1) it is unique for  $A < A_c$ ). We observed the coexistence of two or three types of cycles and the coexistence of chaos and a cycle, for example at  $a = 0.95a_c$ . Thus, the resonance overlapping has already occurred for  $a < a_c$  (i.e., in the invertible region).

At the rest of the present section, some future problems on  $T^3$  will be discussed.

1) In the circle map for  $T^2$ , all tori are stable for  $A < A_c$ , which collapse simultaneously at  $A = A_c$  and chaos appears for  $A > A_c$ . Thus, a dissipative version of a KAM theory can be constructed. How about for  $T^3$ ? There does not seem to exist some critical parameter  $\tilde{a}$  at which chaos appears simultaneously for various values of  $d$ . The construction of a dissipative version of KAM theory, therefore, is not trivial and will be an important problem.

We also note that the resonance overlapping gradually occurs even for  $a < a_c$  for the model of  $T^3$ , while it appears only for  $A > A_c$  for the circle map for  $T^2$ . Detailed study on the relation between the appearance of chaos and the resonance overlapping is left for future.

2) Lockings to tori from  $T^3$  form a double devil's staircase, since they occur when  $R_x/R_y$ ,  $R_x$ , or  $R_y$  is rational, where  $R_x(R_y)$  is a rotation number for the map (4.1). In the case of one-parameter lockings for  $T^2$  in §2, a continued fraction expansion has been a very powerful method for the study of a torus motion. Is it possible to extend the method to the lockings in  $T^3$ ?

3) As is seen in the present section, the onset of chaos seems to occur from a locking to a cycle. In  $T^2$ , a period-doubling cascade from a locking is an essential mechanism for the onset of chaos. In the map (4.1) for  $a < a_c$ , period-doublings of lockings have not yet been observed and they do not seem to be important for the onset of chaos from  $T^3$ . Then, what is the relevant mechanism of the onset of chaos?

It is also important to characterize a chaotic orbit. The notions of ordering and disordering for  $T^2$  are not easily applicable to  $T^3$ ,

because the rotation in the phase space  $(x,y)$  prevents a simple extension of the notions to a  $T^3$ -system, and some new ideas will be necessary. Also, the numerical study on the power spectra for the chaos in the coupled circle map (4.1) has to be performed.

4) In experiments,  $T^3$  (and  $T^4$ ) have been observed in the Rayleigh-Bénard systems<sup>33)-36)</sup>. In these cases, a locking to a lower-dimensional torus is a relevant mechanism for the instability of  $T^3$ , which seems to agree with our numerical results for the previous four-dimensional mappings<sup>30)</sup> and for the present coupled circle map. A unique exception was found by A. Libchaber et al.<sup>35)</sup>, where they studied the convection of mercury in a high magnetic field and observed that the third incommensurate frequency appears simultaneously with an exponentially decaying noise in the low frequency. Thus, the Hopf bifurcation of  $T^2$  seems to lead to chaos, which is rather close to the picture by Ruelle and Takens<sup>1)</sup>. A simple model which explains the above phenomena has to be constructed in future.

5) In connection with the experiments, it will be necessary to construct a "physical" theory for  $T^3$  and chaos. Chaos might exist in the region with small nonlinearity  $a$ . It takes, however, a very long time to distinguish chaos from  $T^3$  and the effect of noise in real systems prevents us from detecting chaos. Thus, we have to construct a theory for the observability of chaos near  $T^3$ , which includes both the time for the observation and the effect of noise.

6)  $T^3$  stably exists. How about  $T^4, T^5, \dots$ , etc.? There is no reason to doubt their existence. The lockings to lower-dimensional tori and to cycles may perhaps play an essential role in such systems, which justify the recent success of a theory of a low-dimensional dynamical system for the onset of chaos. To study such a high-dimensional torus, the author has recently studied the following coupled circle map

$$x_{n+1}(i) = x_n(i) + a \sin(2\pi x_n(i)) + d + b(\sin(2\pi x_n(i+1)) + \sin(2\pi x_n(i-1)) - 2\sin(2\pi x_n(i))), \quad (4.2)$$

where  $i=1,2,\dots,N$  denotes a spatial coordinate of a one-dimensional lattice. The map shows a variety of propagating spatial patterns,

details of which will be shown elsewhere<sup>37)</sup>.

There remains a lot of problems on the chaos from  $T^3$ , which will hopefully be solved in future.

#### Acknowledgement

The author would like to thank Mr. S. Takesue for useful comments and to thank Prof. K. Tomita, Dr. K. Ikeda, and Dr. P. Davis for invaluable comments on  $T^3$ . He is also grateful to LICEPP for the facility of FACOM M190.

#### References

- 1) D. Ruelle and F. Takens, Comm. Math. Phys. 20 (1971) 167; S. Newhouse, D. Ruelle, and F. Takens, Comm. Math. Phys. 64(1978) 35
- 2) S. J. Shenker, Physica 5D (1982) 405
- 3) M.J. Feigenbaum, L.P. Kadanoff, and S.J. Shenker, Physica 5D (1982) 370
- 4) S. Ostlund, D. Rand, J. Sethna and E.D. Siggia, Physica 8D (1983) 303
- 5) K. Kaneko, Prog.Theor. Phys. 68(1982) 669; 69(1983) 403
- 6) L. Glass and R. Perez, Phys. Rev. Lett. 48(1982) 1772; R. Perez and L. Glass, Phys. Lett. 90A (1982) 441
- 7) L. Glass et al., Phys. Rev. A29(1984) No.3; J. Belair and L. Glass, preprint (1984) "Universality and Self-Similarity in the Bifurcations of Circle Maps", submitted to Physica D
- 8) M. Schell, S. Fraser and R. Kapral, Phys. Rev. A28(1983) 1637
- 9) M.H. Jensen, P. Bak, and T. Bohr, Phys. Rev. Lett. 50(1983) 1637 and preprint (1984) "Transition to Chaos by Interaction of Resonances in Dissipative Systems"
- 10) L. P. Kadanoff, J. Stat. Phys. 31(1983) 1
- 11) Preliminary results on the disordering property were reported at the IUTAM conference at Kyoto (1983, September). See K. Kaneko, to appear in **Turbulence and Chaotic Phenomena in Fluids** (North Holland; ed. T. Tatsumi)

- 12) K. Kaneko, preprint "Supercritical Behavior of Disordered Trajectories of a Circle Map" to appear in Prog. Theor. Phys.
- 13) M.J. Feigenbaum, J. Stat. Phys. 19 (1978) 25, 21 (1979) 669
- 14) Y. Pomeau and P. Manneville, Comm. Math. Phys. 74 (1980) 189
- 15) P. Gaspard, Phys. Lett. 97A (1983)1
- 16) C. Grebogi, E. Ott, and J.A. Yorke, Phys. Rev. Lett. 48 (1982) 1507
- 17) For the similar approach to the intermittency problem see Y. Aizawa, Prog. Theor. Phys. 70 (1983) 1249
- 18) see also J. Guckenheimer, Physica 1D (1980) 227
- 19) J. M. Greene, J. Math. Phys. 9(1968) 760, 20(1979) 1183
- 20) K. Kaneko, Prog. Theor. Phys. 69(1983) 1427
- 21) K. Kaneko, Prog. Theor. Phys. 72 (1984) No.2
- 22) K. Kaneko, Prog. Theor. Phys. 71 (1984) 112
- 23) J. P. Sethna and E.D. Siggia, Physica 11D (1984) 193
- 24) A. Arneodo, P. H. Coullet and E.A. Spiegel, Phys. Lett. 94A (1983) 1
- 25) K. Kaneko, Prog. Theor. Phys. 69(1983) 1806
- 26) V. Franceschini, Physica 6D (1983) 285;
- 27) A. Arneodo, preprint (1984) "Scaling for a periodic forcing of a period-doubling system"
- 28) H. Daido, in **Chaos and Statistical Methods**, Springer, 1984 (ed. Y. Kuramoto)
- 29) C. Grebogi, E. Ott and J. Yorke, Phys. Rev. Lett. 51(1983) 339
- 30) K. Kaneko, Prog. Theor. Phys. 71 (1984) 282
- 31) P. Davis and K. Ikeda, Phys. Lett. 100A (1984) 455
- 32) R. K. Tavakol and A.S. Tworkowski, Phys. Lett. 100A (1984) 65 (for 3-torus) and 273 (for 4-torus).
- 33) J. P. Gollub and S. V. Benson, J. Fluid Mech. 100 (1980) 449
- 34) J. Maurer and A. Libchaber, J. Phys. Lett. 41 (1980) L515
- 35) A. Libchaber, S. Fauve and C. Laroche, Physica 7D (1983) 73
- 36) R.W. Walden, P. Kolodner, A. Passner, and C.M. Surko, Phys. Rev. Lett. 53 (1984) 242
- 37) K. Kaneko, to be published in **Dynamical Problems in Soliton Systems**, Springer ; see also K. Kaneko, Prog. Theor. Phys. 72 (1984) No. 3